

Wake studies around a large offshore wind farm using satellite and airborne SAR

M.B. Christiansen^{a,*}, C.B. Hasager^a

^aRisø National Laboratory, Wind Energy Department, Frederiksborgvej 399, P.O. Box 49, DK-4000 Roskilde, Denmark – merete.bruun.christiansen@risoe.dk

Abstract - A method is presented for the mapping of wind speed over the ocean using satellite (ERS-2 SAR, ENVISAT ASAR) and airborne (E-SAR) synthetic aperture radars. Impacts of a large offshore wind farm on the local wind climate are described quantitatively from the radar measurements. Of particular interest is the magnitude and extent of wakes (i.e. regions of reduced wind speed and high turbulence intensity). Results indicate that wind speed reductions in the order of 1 m s^{-1} occur and that wind speed recovers to match the free stream velocity over a downstream distance of $\sim 10 \text{ km}$. This is the minimum spacing that should be recommended between large offshore wind farms in order to limit shadowing and reduced power production.

Keywords: Synthetic aperture radar, ERS-2, ENVISAT, E-SAR, wind energy, wind maps, wake effects.

1. INTRODUCTION

The wind provides a rich energy source, which can be exploited more in order to reach local and global energy targets set up to achieve a sustainable energy supply for years to come and to meet the increasing demand for energy in the world. The recent construction of large wind farms offshore makes wind energy highly acceptable. In addition, energy production increases as larger turbines can be implemented offshore. Current offshore wind farms are installed in near-shore areas where water depths are less than 20 m and where connection to the electrical grid is convenient. Meteorology is complex and not fully understood here due to effects of the coastal discontinuity. Measurements are sparse because the cost of erecting and maintaining an offshore meteorological mast is high.

Synthetic Aperture Radar (SAR) images can be processed to yield ocean wind fields at a relatively low cost. The principle is that small scale roughness at the sea surface is generated instantly by the wind. Backscattering of SAR signals depends on surface roughness. Image brightness is therefore proportional to the local wind speed. The portion of backscatter per area unit is the normalized radar cross section (*NRCS*). Wind speed has previously been derived from SAR with an accuracy of 1.3 m s^{-1} (Hasager et al., 2004). The high spatial resolution of SAR wind speed maps (typically $< 500 \text{ m}$) allows for extraction of wind speed in near-shore areas where wind farms are operating (Monaldo & Kerbaol, 2003). The technique is thus promising in terms of wind energy studies.

This paper presents a study on wake effects of two large offshore wind farms in Denmark. The study is based on wind maps derived from ERS-2 SAR and ENVISAT ASAR satellite scenes. Wind maps are also generated from airborne SAR data acquired over one of the wind farms during a campaign on October 12, 2003.

2. STUDY SITES

An array of 80 wind turbines are operating at Horns Rev in the North Sea, Denmark (<http://www.hornsrev.dk/>). The spacing between individual turbines is 560 m and the distance to shore is 16-20 km. Another wind farm consisting of 72 turbines is located at Nysted in the Baltic where turbines are spaced with 867 m in the east-west direction and 481 m in the north-south direction. The distance to shore is 10-13 km. All turbines have a total height of 110 m above mean sea level.

High quality meteorological measurements are available from a mast located to the north of the wind farm at Horns Rev. Fig. 1 shows the configuration of wind turbines and the meteorological mast. The objects stand out very bright in SAR images acquired under calm conditions.

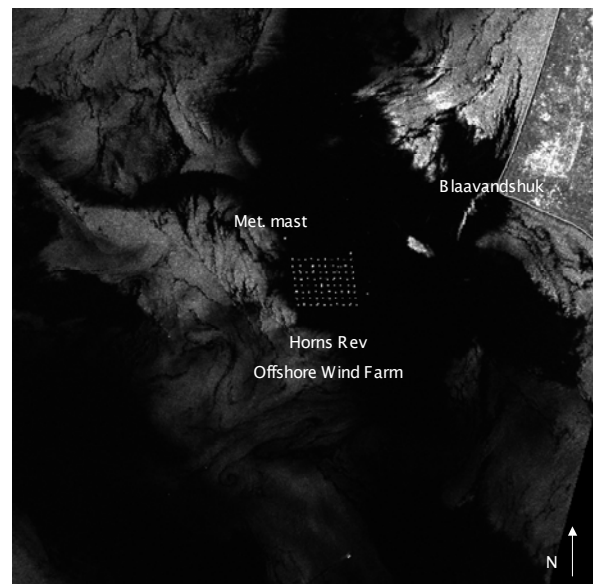


Figure 1. ERS-2 image showing the Horns Rev Offshore Wind farm, Denmark under calm conditions. Bright areas offshore are not associated with the wind.

Two new wind farms named Horns Rev II and Nysted II are planned in the near vicinity of the current wind farms. The precise location of the new wind farms has not yet been determined. There is a tradeoff between the length of cables necessary to connect two wind farms and the potential energy loss due to wake effects.

3. DATA ANALYSIS

3.1 Satellite SAR data

A total of 41 satellite SAR images covering the wind farms at Horns Rev or Nysted have been purchased since the wind farms became operational in 2002 and 2003, respectively. Scenes from the ERS-2 mission are acquired in precision mode and scenes from the ENVISAT mission in either

* Corresponding author

image mode or alternate polarization mode. All of the satellite images have dimensions of ~ 100 km by 100 km and a spatial resolution of 25 m. The radar frequency is 5.3 GHz (C-band) and vertical polarization is used for transmission and reception (VV). Some scenes are contaminated by atmospheric or oceanic noise or the wind speed is too low for turbine operation (< 4 m s⁻¹). After quality control, a total of 19 scenes remain for the study of wakes.

3.2 Airborne SAR data

A flight campaign was conducted over Horns Rev, Denmark by the German Aerospace Research Establishment (DLR) on October 12, 2003. Fig. 2 shows the aircraft used to carry the E-SAR instrument, which operates at several different frequencies and both VV and HH polarization. For the wake study, C-band VV data is chosen. The nominal spatial resolution of E-SAR data is 2 m. Further details on the E-SAR system are available at http://www.op.dlr.de/ne-hf/projects/ESAR/esar_englisch.html.



Figure 2. Dornier DO 228 aircraft used for acquisition of E-SAR data over Horns Rev, Denmark on October 12, 2003.

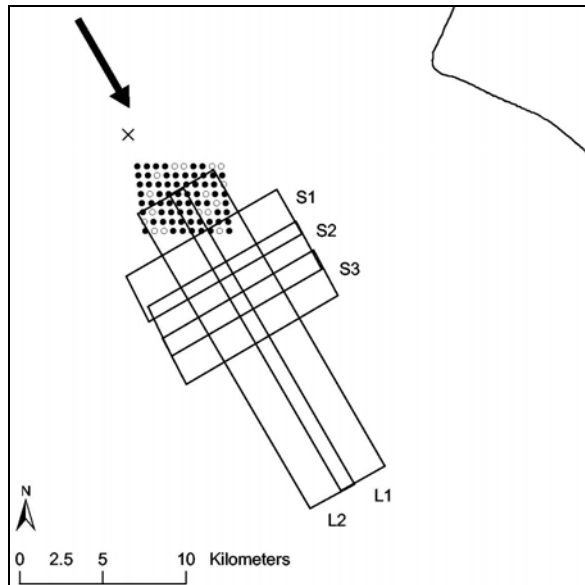


Figure 3. Configuration of E-SAR flight tracks acquired in C-band VV. Arrow indicates wind direction (330°), x the met. mast, and dots are wind turbines (filled if running).

E-SAR data were acquired as five tracks downstream of the Horns Rev Offshore Wind Farm as shown in Fig. 3. Two tracks (L1-L2) are aligned with the wind direction and ~ 20 km long. Three shorter tracks (S1-S3) of ~ 10 km are acquired perpendicular to the wind. All tracks are 3 km wide, which corresponds to incidence angles of 26-55°. Meteorological measurements of wind direction and wind speed at times corresponding to the E-SAR acquisition are shown in Table 1.

Table 1. Meteorological measurements of wind direction and wind speed during E-SAR campaign.

Track	Start time	End time	Wind dir.	Wind speed
L1	8:31:21	8:35:25	338	10.6
L2	8:47:12	8:51:09	340	9.4
S1	9:28:50	9:30:47	342	11.0
S2	10:06:59	10:08:52	325	9.2
S3	10:18:59	10:20:56	325	8.5

3.3 SAR wind speed retrieval

All the SAR scenes are calibrated to NRCS. In order to reduce speckle noise and effects of longer period internal waves, averaging of grid cells is necessary. It is conventional to use a grid cell size of 400-500 m for SAR wind speed retrievals. In the present study, it is crucial to maintain a higher spatial resolution in order to distinguish single wind turbines in the satellite and airborne SAR images. To compensate for the higher noise level, wind speeds are obtained as spatial averages from the resulting wind speed maps.

Empirical algorithms describe the backscatter-to-wind relationship for SAR images. For example, the CMOD-4 algorithm developed by Stoffelen & Anderson (1997) is:

$$NRCS = U^\gamma (a_0 + a_1 \cos \phi + a_2 \cos 2\phi) \quad (1)$$

where $NRCS$ = normalized radar cross section
 U = wind speed
 Φ = wind direction relative to look direction
 a_0, a_1, a_2 and γ = coefficients depending on incidence angle and wind speed

As seen from Eq. 1, it is necessary to know the wind direction in order to retrieve wind speed from CMOD-4. In our case, wind directions are obtained from the meteorological mast at Horns Rev assuming a uniform direction for each entire SAR image. The *in situ* measurements are obtained as 10 minute averages whereas satellite images are instant snap-shots. E-SAR data are acquired over 2-4 minutes per flight track.

Due to fluctuations of the wind direction, deviation may occur between *in situ* measurements and directional indicators such as wind streaks in the SAR images. The direction indicated by streaks is then considered appropriate as CMOD-4 input. We invert Eq. 1 to obtain maps of wind speed.

4. RESULTS

4.1 Velocity deficit from satellite SAR

Reductions of wind speed due to turbine wake effects are described as velocity deficit:

$$VD = \frac{U_{freestream} - U_{wake}}{U_{freestream}} 100\% \quad (2)$$

where VD = velocity deficit
 U = wind speed

The classical approach in meteorology is to obtain $U_{freestream}$ upstream and U_{wake} downstream of wind turbines. Using an upstream source of reference may be problematic in near-shore areas due to general changes of wind speed with distance offshore (e.g. speed-up effects with offshore winds). Meteorological measurements are usually obtained as averaged time series.

Satellite winds are acquired instantly and averaged in space. This allows us to reference wind speeds obtained in a transect of boxes upstream, through and downstream of a wind farm to wind speeds obtained in an identical transect in the non-obstructed wind flow. Fig. 4 shows an example wind map based on an ERS-2 SAR scene acquired on October 12, 2003. Shades of gray indicate variations of wind speed. Superimposed on the wind map are two transects of boxes aligned with the wind direction. Spatial means of wind speed are obtained within each box and used for calculation of VD . Extreme $NRCS$ values caused by wind turbines are removed prior to averaging of grid cells.

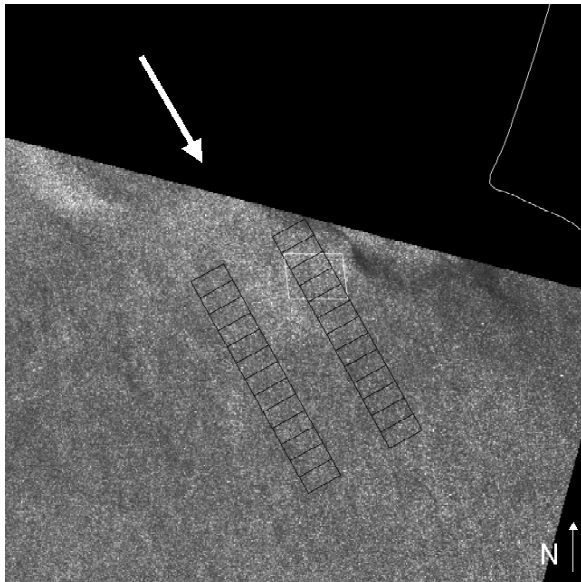


Figure 4. Grayscale ($0-15 \text{ m s}^{-1}$) wind speed map, ERS-2 SAR, October 12, 2003. Wind dir. 330° (arrow). Wind farm (white trapezoid) and transects (black boxes) are indicated.

Average VD for the 19 satellite SAR scenes covering the wind farm at Horns Rev or Nysted are shown in Fig. 5. Results are combined for onshore winds, offshore winds and all scenes, respectively. Positive values of VD indicate that measured wind speeds are below the reference velocity.

Velocity deficits up to 10% are found 0-3 km downstream of the wind farms. At the downstream distance 10 km, VD is $\sim 4\%$ on average. The distribution of VD is similar for onshore and offshore winds due to the alternative reference method used.

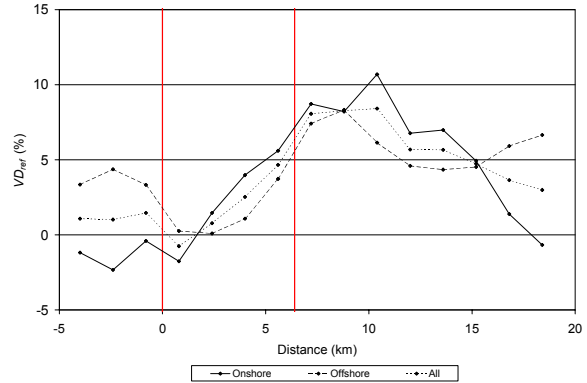


Figure 5. Average velocity deficit obtained from a total of 19 satellite SAR wind maps. Vertical lines indicate maximum wind farm boundaries.

4.2 Wind speed variations from airborne SAR

Figure 6 shows wind speed in grayscale for the E-SAR track L1. E-SAR flight tracks are obtained downstream of the wind farm at Horns Rev and non-obstructed reference measurements are thus not available. An additional complexity is that individual tracks are acquired at different times during the 3-hour E-SAR campaign. As seen in Table 1, wind speed and direction fluctuates and a trend of decreasing wind speed is observed.

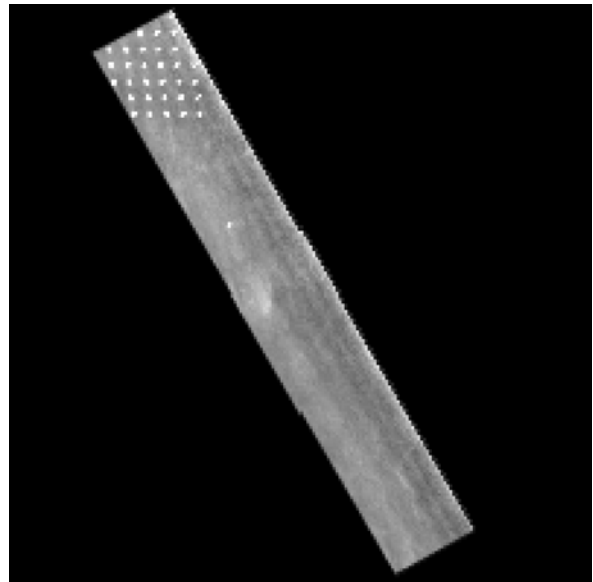


Figure 6. Wind speed for the E-SAR track L1. Wind turbines and a ship are seen as very bright pixels. This image noise is removed with a mask.

Results from the E-SAR campaign are interpreted as absolute values. An example for a long flight track (L1) is shown in Fig. 7. The plot shows a general decrease of wind speed with downstream distance but with large fluctuations. The flight track contains some of the wind turbines at Horns

Rev. High scattering from the turbines is removed through application of a mask and the plots show how wind speed is reduced over the wind farm after the correction.

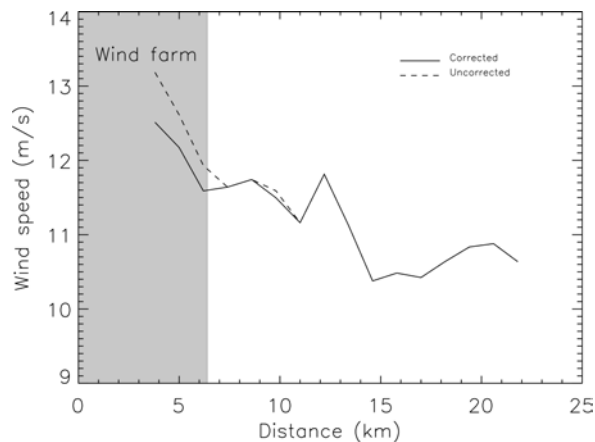


Figure 7. Wind speed along E-SAR track L1. Results are shown before and after correction for turbine scattering.

Wind speeds obtained along the short flight tracks (S1-S3) are shown in Fig. 8. A significant reduction of wind speed ($\sim 2 \text{ m s}^{-1}$) is observed downstream of the wind farm center for S1 and S3. For S2, a similar variation of wind speed is seen, however, the minimum is shifted by 1-2 km.

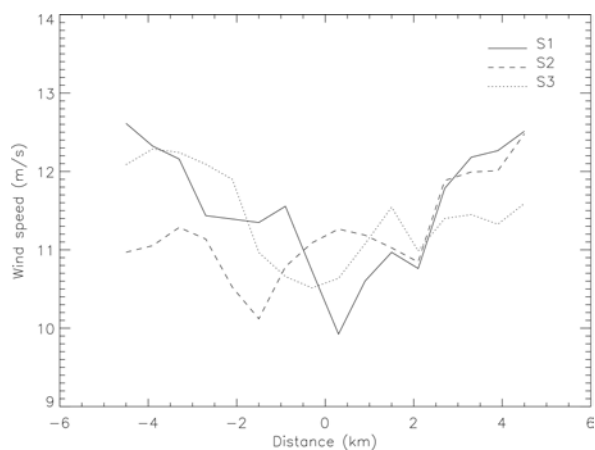


Figure 8. Wind speed obtained for short E-SAR tracks (S1-S3). Distances of 0 km are downstream of wind farm center.

5. DISCUSSION

Wind maps derived from satellite SAR are very useful in wake studies. The availability of data from numerous locations in space allows for calculation of velocity deficit through a new, alternative approach. In near-shore areas, this method is superior to the classical meteorological approach of using upstream measurements as reference. Results from satellite SAR indicate that wind wakes are persistent over the entire downstream distance studied ($\sim 10 \text{ km}$). This is consistent with model predictions (Barthelmie et al., 2004). The persistency of wind wakes in time and space depends on atmospheric stability. Christiansen & Hasager (2005) has found a longer persistency in SAR images acquired under stable or near-neutral atmospheric conditions compared to unstable conditions. Maximum velocity deficits are found for wind speeds of $8\text{-}10 \text{ m s}^{-1}$ (Frandsen & Hauge Madsen, 2003).

Results from airborne SAR show a general decrease of wind speed with distance downstream of the wind farm at Horns Rev. Short tracks acquired perpendicular to the wind direction confirm that wind speed reductions are due to wake effects of the large offshore wind farm. Minimum wind speed is observed close to the wind farm (S1). Shifting locations of the minimum wind speed for the three short tracks may result from fluctuations of wind direction. The accuracy of E-SAR calibration is low (2 dB) compared to the accuracy of satellite SAR measurements (0.2 dB). Some uncertainty is added during wind speed retrievals from CMOD-4. The major advantage of the E-SAR data is the high spatial resolution.

6. CONCLUSION

It has been demonstrated that the extent and magnitude of wind wakes downstream of large offshore wind farms can be identified from satellite and airborne SAR. Velocity deficits of $\sim 10\%$ are found downstream of the wind farms and the wake persistency is at least 10 km. The results are consistent with wake models.

ACKNOWLEDGEMENTS

Funding for the study was provided through the SAR-WAKE project (26-02-0312), Danish Technical Research Council (STVF). The satellite images are granted from the European Space Agency in Cat. 1 project EO-1356. Elsam Engineering A/S is thanked for meteorological and production data.

REFERENCES

- Barthelmie, R.J., Pryor, S.C., Frandsen, S. & Larsen, S. (2004). Analytical and empirical modelling of flow downwind of large wind farm clusters. In *Special Topic Conference: The science of making torque from wind, Delft (NL)*, pp. 292-303.
- Christiansen, M.B. & Hasager, C.B. (2005). Wake effects of large offshore wind farms identified from satellite SAR. *Remote Sensing of Environment*, submitted.
- Frandsen, S., & Hauge Madsen, P. (2003). Spatially average of turbulence intensity inside large wind turbine arrays. In *Offshore wind energy in Mediterranean and other European seas. Resources, technology, applications. OWEMES 2003. European seminar, Naples (IT)*, pp. 97-106.
- Hasager, C.B., Dellwik, E., Nielsen, M. & Furevik, B. (2004). Validation of ERS-2 SAR offshore wind-speed maps in the North Sea. *International Journal of Remote Sensing*, 25: 3817-3841.
- Monaldo, F., & Kerbaol, V. (2003). The SAR measurement of ocean winds: An overview for the 2nd workshop on coastal and marine applications of SAR. *Proceedings of the Second Workshop on Coastal and Marine Applications of SAR, Svalbard (N)*. CD-ROM.
- Stoffelen, A. & Anderson, D.L.T. (1997). Scatterometer data interpretation: Estimation and validation of the transfer function CMOD4. *Journal of Geophysical Research*, 102: 5767-5780.